Insights into Effects of Surfactant Concentration on Foam Behavior in Porous Media

Kahrobaei, S.; Farajzadeh, R.

Important note
To cite this publication, please use the final published version (if applicable).
Please check the document version above.

Insights into Effects of Surfactant Concentration on Foam Behavior in Porous Media

S. Kahrobaei[†,‡] and R. Farajzadeh*[,†,§]

†Delft University of Technology, Delft 2628 BC, The Netherlands
‡Currently with TNO, Utrecht 3584 CB, The Netherlands
§Shell Global Solutions International B.V., Rijswijk 2288 GS, The Netherlands

ABSTRACT: A potential solution to mitigate the adverse effects of viscous fingering, gravity override, and reservoir heterogeneity on the efficiency of gas injection in porous media is to inject the gas with a solution containing surface-active agents such as surfactants or nanoparticles. The efficiency of these processes largely depends on the generation and stability of the lamellae residing in the pores, both of which are influenced by the physicochemical properties of the rock and the surfactant solution. This study investigates the effect of surfactant concentration on the transient and steady-state behaviors of foam in porous media. It is found that the rate of foam generation is affected by the surfactant concentration, i.e., the transition from coarse-textured to fine-textured (strong) foam occurs earlier with the increasing surfactant concentration. However, when a sufficient amount of the surfactant is injected, strong foam is generated even with a very low surfactant concentration in the low-quality regime. Furthermore, because foam stability is governed by the limiting capillary pressure in the high-quality regime, the steady-state pressure behavior of foam (or foam strength) in this regime is significantly impacted by the surfactant concentration. We find that the current (equilibrium or steady-state) foam models cannot mimic the observed behavior in our experiments because it scales both high- and low-quality regimes with the surfactant concentration. Consequently, modifications are suggested to overcome the shortcomings of the model.

1. INTRODUCTION

A potential solution to mitigate the adverse effects of viscous fingering, gravity override, and reservoir heterogeneity on the efficiency of gas injection in porous media is to inject the gas with a solution containing surface-active agents such as surfactants[1−5] or nanoparticles.[6,7] Upon mixing of the surfactant solution, the gas foam films (lamellae) are formed, which create resistance against the gas flow and thus increase the magnitude of the viscous forces against the gravity and capillary forces. Therefore, the success of a foam injection process largely depends on the generation and stability of the lamellae residing in the pores, both of which are influenced by the physicochemical properties of the rock and the surfactant solution.

Foam coalescence in porous media is dictated by the magnitude of the capillary pressure, i.e., the difference between the gas and liquid pressures. Above a certain capillary pressure (known as the limiting capillary pressure or P_c^*), the rate of lamellae rupture increases significantly and foam texture (the number of lamella per unit volume) becomes coarser. P_c^* (and hence foam coalescence rate) varies with the rock permeability, surfactant type, and concentration, among other parameters. In particular, it has been inferred from experimental data that the value of P_c^* increases with the increase in the surfactant concentration.[8−10] This indicates that the foam coalescence rate increases as the surfactant concentration decreases. Aronson et al.[11] demonstrated that the surfactant solutions with higher repulsive critical disjoining pressure, Π, (i.e., solutions with a high surfactant content) lead to more stable foams in porous media. In the view of these experiments, they

asserted that P_c^* is directly related to the critical disjoining pressure, Π^{cr}.

The influence of the surfactant concentration on foam generation in porous media is more ambiguous. At least, in the proposed foam-generation mechanisms (snap-off, lamellae division, and leave behind), there are no explicit functionalities that account for the surfactant-concentration effect. For example, snap-off generates bubbles as long as water saturation is high and capillary pressure is low regardless of the surfactant concentration.[10] However, the survival of the generated lamellae strongly depends on the surfactant concentration. In other words, occurrence of snap-off is not sufficient for the formation of strong foam. For foam generation by lamella-division, the lamella must also remain stable until it meets the next obstacle and splits in two different lamellae. The stability of initial foam (or liquid lenses) is a necessary condition for attaining the minimum pressure gradient required for strong foam generation in porous media. Therefore, foam generation in porous media is expected to be an implicit function of the surfactant concentration, although the effect is not strong for the concentrations above the critical micelle concentration (CMC).[12] Jones et al.[13] observed a transition at the CMC in the bulk foam, i.e., the foam strength remained unaffected by a further increase of the surfactant concentration. Nevertheless, in the porous-media experiments, the maximum "apparent viscosity" (defined by eq 1) experienced a gradual rise with the increase in the surfactant concentration. This was attributed
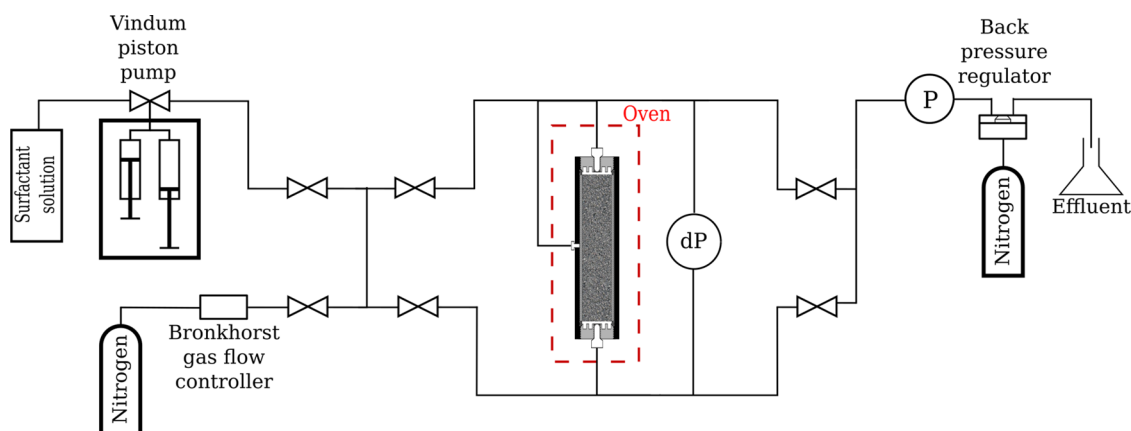
Figure 1. Schematic of the experimental apparatus.

partly to the surfactant depletion from the bulk liquid to the gas/water interfaces of foam bubbles, which appears to be more significant in porous-media foam than in the bulk foam due to a larger surface area. This reduces the effective surfactant concentration in the aqueous phase, which in turn affects the number of stable foam films or lamellae. Jones et al.[13] estimated that in their porous-media foam the amount of the surfactant depleted to the gas/water interface was about 5 times the CMC (10 times more than that of the bulk foam). Hirasaki and Lawson[2] suggested that during foam flow the surfactant depletes at the front and accumulate at the back, resulting in a surface-tension gradient that resists flow and increases the effective viscosity. As a result, the displacement efficiency of foam increases with the increasing surfactant concentration.[10]

The steady-state rheology of foam in porous media is tuned by the gas fractional flow or foam quality, f_g. At lower gas fractional flows (or in the low-quality regime), the strength of foam is mainly determined by the gas velocity, whereas at higher gas fractional flows (or in the high-quality regime), liquid velocity plays the dominant role in determining the equilibrium foam texture. It is our objective to investigate the effect of the surfactant concentration on foam behavior in both high- and low-quality regimes in porous media. We performed experiments in which nitrogen and a surfactant solution (with varying concentration) were simultaneously injected into a core with different ratios at a constant total flow rate. Moreover, the ability of the current foam models in simulating the effect of surfactant concentration was examined and modifications were suggested accordingly.

The structure of the paper is as follows: Section 2 describes the experimental methodology and material used. Section 3 presents and discusses the experimental results. In Section 4, the experimental results are modeled and some modifications to the current foam models are proposed. Finally, the paper ends with the concluding remarks.

2. EXPERIMENTS

2.1. Chemicals and Materials. In the first series of experiments, α olefin sulfonate (AOS) C_{14-16} (Stepan BIO-TERGE AS-40 KSB) was used as the foaming agent. The properties of the foam films stabilized by this surfactant can be found in ref 14. The NaCl concentration was fixed to 1.0 wt % ($\sim$0.17 M) in all experiments. The critical micelle concentration (CMC) of the AOS surfactant in demineralized water with 1 wt % of NaCl was measured as 0.008 wt % using the Du Noüy ring method. Five different AOS concentrations,

ranging from 0.008 to 1.5 wt %, were used to study the effect of surfactant concentration on foam flow behavior. In the second series of the experiments, internal olefin sulfonate (IOS15-18) (Shell Chemicals) was used as the foamer. The CMC of the IOS surfactant in the demineralized water with 1 wt % of NaCl was measured to be 0.01 wt %. Four different IOS concentrations, ranging from 0.1 to 1.5 wt %, were used to study the effect of the surfactant type on the foam behavior. Nitrogen (N_2) with a purity of 99.98% was used as the gas phase in our experiments. A 17 cm cylindrical quasi-homogenous Bentheimer sandstone core with a diameter of 3.8 cm was used as the porous medium. The average porosity of the core was 0.23. The permeability of the core was measured to be 2.3×10^{-12} m^2 ($\pm$0.005 $\times 10^{-12}$ m^2).

2.2. Experimental Setup. The schematic of the experimental apparatus is shown in Figure 1. The core sample was vertically placed inside a cylindrical core-holder and was located inside an oven to keep the temperature constant at 30 °C. The gas flow rate was controlled using a calibrated Bronkhorst mass-flow controller. The surfactant solution was injected at a constant rate using a Vindum double-effect piston-displacement pump. The overall pressure difference along the core was measured using a differential pressure transducer connected to the input and the output lines of the core-holder. A back-pressure regulator was connected to the outlet of the core to maintain a constant pressure of 25 bar at the core outlet. The accuracy of the pressure transducers is 1 mbar. All of the measurement instruments were connected to a data acquisition system to record data with a frequency of 5 s.

2.3. Experimental Procedure. After a leak test, 10 pore volumes of CO_2 were injected into the core to remove the air from the core. The procedure was continued by vacuuming the core. Afterward, CO_2 was dissolved and the procedure was carried out by injecting brine at an elevated pressure (25 bar). Subsequently, the core permeability was calculated by measuring the pressure drop along the core at different brine flow rates using Darcy's law. Then, the core was presaturated with the surfactant solution to satisfy the surfactant adsorption on the rock.

The so-called foam quality experiments[15,16] were conducted to study foam flow in porous media. In these experiments, the gas and the surfactant solution are coinjected at a constant total rate into the rock until the steady-state pressure is reached. For all volume fractions, the gas phase and the surfactant solution were coinjected with a constant total flow rate of 1.0 mL/min, corresponding to a total superficial velocity of 1.4×10^{-5} m/s. The coinjection was continued until the steady-state pressure was obtained for the respective gas fractional flow. Subsequently, the gas volume fraction was altered and the system was allowed to reach a new steady state. The gas volume fractions were altered randomly to minimize the effect of the previously established state on the results. After completion of a foam-quality-scan experiment, the core was cleaned using propanol solution and the trapped air was removed by CO_2 injection and consequent vacuuming. Subsequently, the permeability was measured to ensure

similar initial conditions for the next experiment. Table 1 provide a summary of the foam-quality-scan experiments using AOS and IOS surfactants.

Table 1. Summary of the Experiments with Two Surfactant Types

experiments with AOS		experiments with IOS	
experiment no.	surfactant concentration [wt %]	experiment no.	surfactant concentration [wt %]
AOS-1	0.008	IOS-1	0.1
AOS-2	0.1	IOS-2	0.5
AOS-3	0.5	IOS-3	1
AOS-4	1	IOS-4	1.5
AOS-5	1.5		

The apparent viscosity of the flowing foam is calculated using single-phase Darcy's law and the measured steady-state pressure drops

$$\mu_{app} = \frac{kA}{q_g + q_l} \frac{|\Delta p|}{L} \tag{1}$$

where k [m^2] is the absolute permeability, A [m^2] is the cross-sectional area, q_g [m^3/s] and q_l [m^3/s] represent the flow rates of the gas phase and the surfactant solution (liquid phase), respectively, and Δp [Pa] is the pressure drop along the core length, L [m]. Moreover, the fractional flow of the gas phase or foam quality (f_g) is defined by

$$f_g = \frac{q_g}{q_g + q_l} \tag{2}$$

The error bars for each data point were calculated using the standard deviation of the steady-state-pressure measurements.

3. RESULTS AND DISCUSSION

3.1. Transient Behavior. Each foam-quality-scan experiment started with a foam-generation phase, i.e., in the beginning of each experiment, there was no foam in the porous medium. The experiments started with a foam quality of 0.30 or 30% gas fraction. Figure 2a shows the pressure history of the foam-generation phase of the experiments for

different AOS concentrations at a fixed foam quality of 0.30. Figure 2b magnifies the first four pore volumes of the injection. It can be seen that, for a certain foam quality, as the surfactant concentration increases the jump in the pressure history starts earlier. The jump in the pressure gradient is interpreted as the transition from coarse-textured foam to strong or fine-textured foam.[17] For the highest surfactant concentration (1.5 wt %), the jump in the pressure gradient occurs at 0.4×10^5 Pa/m after 1.4 pore volumes of injection and reaches the steady-state condition after 8 pore volumes of injection. These values are provided in Table 2 for other experiments.

Table 2. Pressure Gradient for Transition from Coarse-Textured to Fine-Textured Foam and Its Corresponding Total Injected Pore Volume

| AOS concentration [wt %]	transition pressure gradient [Pa]	transition pore volume [-]	steady-state pore volume [-]
0.008	$0.4-1.0 \times 10^5$	7	80
0.1	0.4×10^5	1.4	24
1	0.4×10^5	1.4	18
1.5	0.4×10^5	1.4	8

At the CMC, the pressure gradient increases gradually from 0.4×10^5 to 1×10^5 Pa/m between 1 and 7 pore volumes of injection. Thereafter, the pressure gradient increases with a greater slope followed by a jump after 48 pore volumes of injection. Finally, it reaches the steady-state condition after 80 pore volumes of injection. Based on the steady-state pressure data, it can be concluded that foam generation is independent of the surfactant concentration. For the concentrations above the CMC, the transition from coarse foam to strong foam occurs at the same pressure gradient of 0.4×10^5 Pa/m. In other words, the minimum pressure gradient required for foam generation is independent of the surfactant concentration. Once the minimum pressure gradient is reached, the rate of foam generation strongly depends on the surfactant concentration. This is likely related to the net rate of lamellae creation
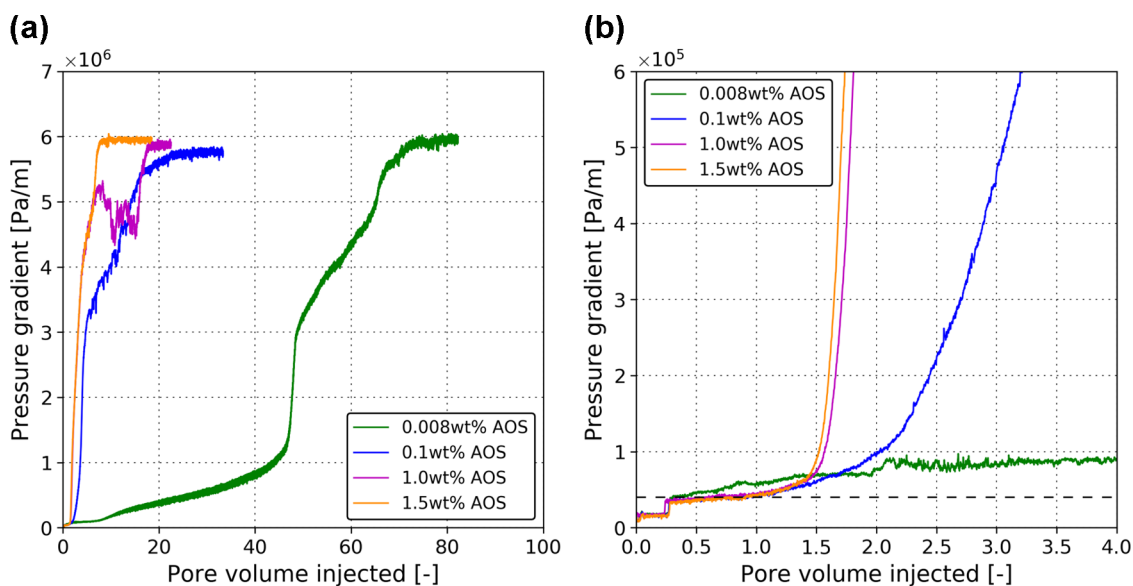
Figure 2. (a) Pressure history of the foam-generation phase of the experiments with a gas volume fraction (foam quality) of 0.30 for different AOS concentrations. (b) Magnification of the first four pore volumes of injection.
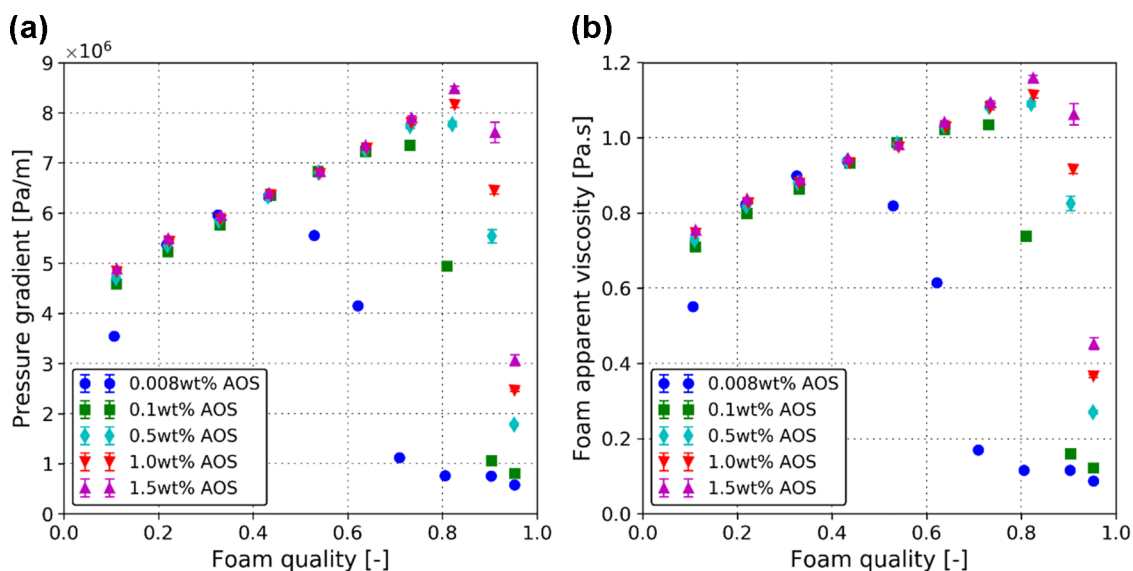
Figure 3. (a) Steady-state pressure gradient along the core and (b) calculated apparent viscosity at different foam qualities (gas fractional flow) using eq 1 for different AOS concentrations. The total flow rate was set to a constant value of 1 mL/min.
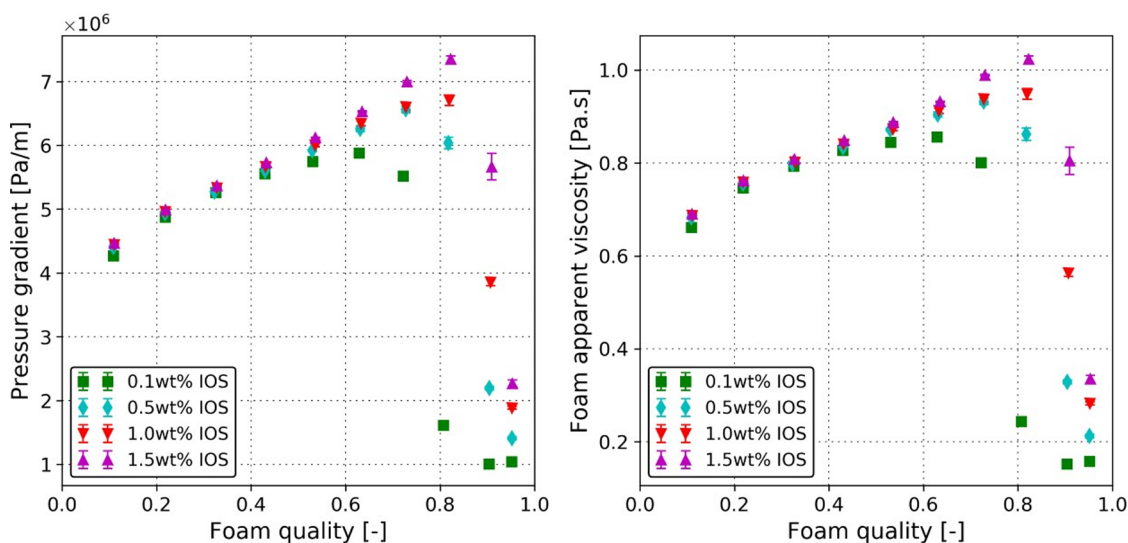
Figure 4. (a) Steady-state pressure gradient along the core and (b) calculated apparent viscosity at different foam qualities, f_g, for different IOS concentrations. The total flow rate was set to a constant value of 1 mL/min.

and destruction. As the surfactant concentration decreases, more pore volume of injection is required for lamellae creation to exceed the foam destruction. In the high-quality regime, even after many injected pore volumes, the transition to strong foam may not occur and the generated foam may remain weak. This is because the created lamellae are unstable due to dominance of the limiting capillary pressure.[17]

3.2. Steady-State Behavior. Figure 3a,b shows the measured steady-state pressure gradient and the calculated apparent viscosity at different foam qualities for different AOS concentrations, respectively. In all experiments, the apparent foam viscosity increases with the increasing foam quality (low-quality regime) and then above a certain foam quality (referred to as transition foam quality, f_g^{tr}) it starts to decrease (high-quality regime).

Figure 3 exhibits the remarkable effects of the surfactant concentration on foam rheology in porous media. First, in all experiments, both foam qualities appear to exist; however, as

the surfactant concentration increases, the transition from the low- to high-quality regime occurs at a larger foam quality. For example, the transition foam quality increases from 0.43 to 0.82 when the surfactant concentration increases from 0.008 to 1.5 wt %. Above the surfactant concentration of 0.5 wt %, the increase in the transition foam quality becomes marginal, such that its quantification becomes difficult as the difference falls within the accuracy of our measurements.

Second, the surfactant concentration affects only the high-quality regime. In the low-quality regime, the apparent viscosity of foam is independent of the surfactant concentration. However, the transition foam quality and its corresponding apparent foam viscosity increase with the surfactant concentration. Consequently, in the high-quality regime, foam becomes stronger (or foam texture becomes finer) as the surfactant concentration increases. This is because in the high-quality regime foam stability depends on P_c^*, whose value increases with the increasing surfactant concen-

tration.[9,10,17] The maximum foam apparent viscosity increases from 0.93 Pa s (with 0.008 wt % AOS) to 1.15 Pa s (with 1.5 wt % AOS). However, for the concentrations above 0.50 wt %, the difference in the maximum foam apparent viscosity becomes less pronounced. No foam was observed in the effluent with 0.90 and 0.95 foam qualities and 0.008 wt % AOS concentration. Although this behavior can be due to the instability of foam films when they leave the cores, their high foam apparent viscosity value ($\sim$0.1 Pa s) might also be because of the remaining foam from the previously established state. Moreover, for the experiment with f_g = 0.1 (with 0.008 wt % AOS), the experiment stopped before establishing a steady state.

To investigate the effect of the surfactant type and to ensure that the observed behavior is not limited to the AOS surfactant, more foam-quality-scan experiments were conducted with a different surfactant formulation. Figure 4a,b shows the measured steady-state pressure gradient and the calculated apparent viscosity at different foam qualities for different IOS concentrations, respectively.

Similar to the experiments with the AOS surfactant, the variation in the IOS surfactant concentration affects only the high-quality regime. The transition foam quality increases from 0.62 (with 0.1 wt % IOS) to 0.82 (with 1.5 wt % IOS). Moreover, the maximum foam apparent viscosity increases from 0.82 Pa s (with 0.1 wt % IOS) to 1.02 Pa s (with 1.5 wt % IOS).

4. SIMULATION OF STEADY-STATE FOAM BEHAVIOR

4.1. Implicit-Texture (IT) Foam Model. The current foam models assume that the presence of foam affects only the gas mobility, whereas the liquid phase mobility remains unaffected.[3,18,19] In the implicit-texture (IT) or local-equilibrium foam model, the gas mobility-reduction factor is calculated through several functions depending on variables such as phase saturation, surfactant concentration, superficial velocities, etc.[9,15,16,20]

$$\lambda_g^f = \lambda_g^{nf} FM = \frac{\lambda_g^{nf}}{1 + fmmob F_1 F_2 F_3 F_4 F_5 F_6}$$

$$= \frac{K k_{rg}^{nf}(S_w)/\mu_g}{1 + fmmob F_1 F_2 F_3 F_4 F_5 F_6} \qquad (3)$$

where λ_g^f [-] and λ_g^{nf} [-] are gas mobilities in the presence and absence of foam, respectively. k_{rg}^f [-] is the gas relative permeability in the presence of foam. fmmob [-] is the maximum mobility-reduction factor. The F_i [-] functions are dimensionless with a value between 0 and 1. Each F_i function corresponds to a different parameter; for example, F_1, F_2, F_3, F_4, F_5, and F_6 represent the effect of surfactant concentration, water saturation, oil saturation, shear-thinning behavior, gas velocity, and critical capillary number on foam rheology in porous media, respectively.[20,21,24]

In this study, we focus on the effect of the surfactant concentration (F_1), water saturation (F_2), and shear-thinning (F_5) functions. The surfactant concentration function is defined as

$$F_1 = \begin{cases} \left(\dfrac{C_s}{fmsurf}\right)^{epsurf} & , C_s < fmsurf \\ 1 & , C_s \geq fmsurf \end{cases} \qquad (4)$$

where C_s [wt %] is the surfactant concentration, fmsurf [wt %] is the critical surfactant concentration above which gas mobility is independent of the surfactant concentration, and epsurf [-] is a parameter that regulates the foam strength for surfactant concentrations below fmsurf. The F_2 function is defined as

$$F_2 = 0.5 + \frac{\arctan(epdry(S_w - fmdry))}{\pi} \qquad (5)$$

where fmdry [-] is equivalent to the limiting water saturation and epdry [-] controls the abruptness of transition from high- to low-quality regimes. Large values of epdry result in a sharp transition, i.e., foam collapses within a very narrow range of water saturation (see ref 9 for more explanation). The shear-thinning function is defined as

$$F_5 = \left(\frac{fmcap}{N_{Ca}}\right)^{epcap} \qquad (6)$$

where epcap [-] is the shear-thinning exponent and fmcap [-] is the reference rheology capillary number. Capillary number is defined as

$$N_{Ca} = \frac{k\nabla p}{\sigma} \qquad (7)$$

where ∇p [Pa/m] is the pressure gradient and σ [N/m] is the surface tension.

Foam-model parameters are estimated by minimizing an objective function, which is defined as a mismatch between simulated data and experimental data. Corey-type relative permeabilities[22] are used for gas and water relative permeability functions, and the water saturation, S_w, is back-calculated from steady-state pressure data using the parameters provided in Table 3 taken from ref 19.

Table 3. Fluid Properties and Relative Permeability Data

parameter	value	unit
μ_w	0.810×10^{-3}	Pa s
S_{wc}	0.05	
S_{gr}	0.03	
n_w	4.42	
n_g	0.94	
k_{rw}^0	0.72	
k_{rg}^0	0.59	
σ_{wg}	0.03	N/m

In the estimation of the foam-model parameters, the gas viscosity (μ_g) and the total velocity (u_t) are corrected for each experimental data point using the Peng−Robinson equation of state[23] at the corresponding experimental pressure and temperature.
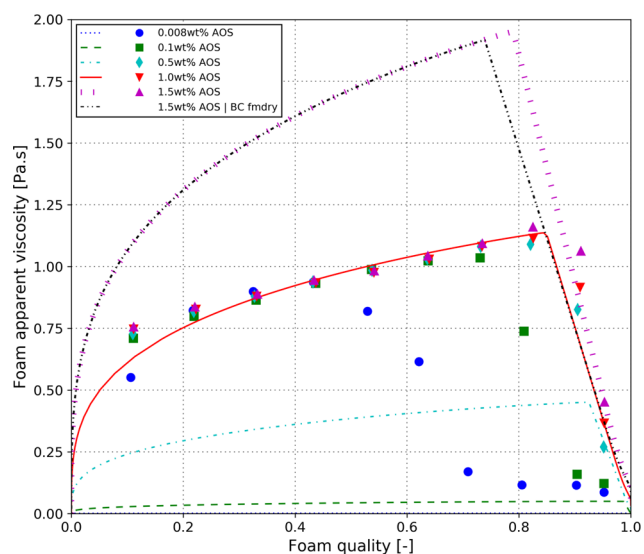
4.2. Modeling the Effect of Surfactant Concentration on Steady-State Foam Behavior. In the IT foam model, it is assumed that for a given surfactant formulation the set of the foam-model parameters is unique and the effect of surfactant concentration is reflected by the C_s value in the F_1 function. The first difficulty in representation of foam physics by eq 4 is the determination of fmsurf, i.e., the surfactant concentration above which the foam strength remains unaffected. However, this concept might only be true for the bulk foam. In fact, in the porous-media foam, the maximum apparent viscosity keeps increasing with the addition of surfactant, as shown in Figures

3 and 4. In this study, the fmsurf is assumed to be 2.0 wt % and the experiments data of 1.0 wt % is used as the base case to estimate the foam-model parameters, x = [fmmob, fmdry, fmcap, epcap, epsurf], presented in Table 4. It is noted that

Table 4. Foam Model Parameters for the Base Case Using F_1, F_2, and F_5 Functions

parameter	value
fmmob	1.10×10^6
fmdry	0.1755
epdry	1×10^5
fmcap	0.0005
epcap	2.26
fmsurf	2
epsurf	4.537

changing only the F_1 function results in different foam strengths in the low-quality regime (see the 1.5 wt % AOS curve in Figure 5 calculated with the same fmdry value as in
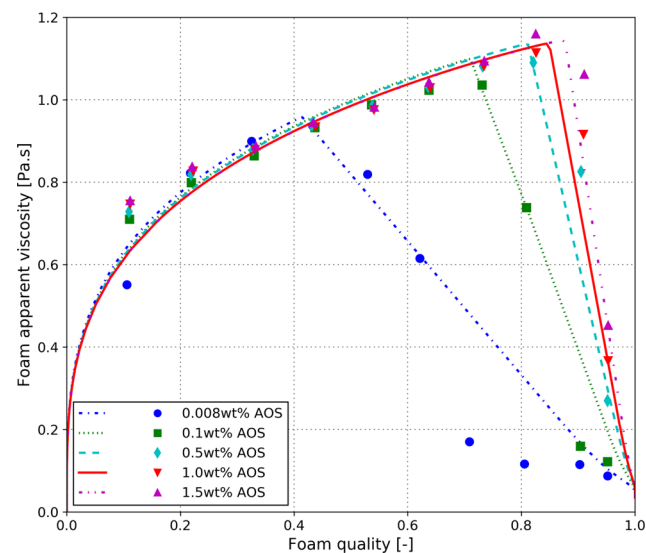

Figure 5. Modeling of foam apparent viscosity using F_1, F_2, and F_5 functions assuming a constant set of parameters (Table 5) but different values of C_s and fmdry (Table 6) to capture the effect of surfactant concentration. The dashed-dotted-dotted line shows the 1.5 wt % AOS case using the same fmdry value as in the base case.

the base case as an example). Therefore, to account for the changes in the high-quality regime, the fmdry parameter needs to be varied for different surfactant concentrations as well. With these assumptions, the fit to the experimental data is shown in Figure 5.

Figure 5 reveals the second issue with the description of the surfactant effect using eq 4. Based on this formulation, as the surfactant concentration increases, foam apparent viscosity increases in both low- and high-quality regimes, which is in contrast with our findings in Figures 3 and 4 that the surfactant concentration affects only the high-quality regime by changing the limiting capillary pressure or the corresponding water saturation. Hence, the effect of surfactant concentration on foam behavior can be implicitly modeled by a concentration-dependent fmdry parameter in the F_2 function and the F_1 function can be removed from the steady-state IT foam models. The results of such an approach are plotted in Figure 6

using the parameters in Tables 5 and 6. The small deviations in the low-quality regime in Figure 6 are because of the minor differences in the corrected velocities.

Figure 6. Simulation of the experimental data using F_2 and F_5 functions assuming constant set of parameters (Table 5) but different values of fmdry (Table 6) to capture the effect of surfactant concentration.

Table 5. Foam Model Parameters for the Base Case Using F_2 and F_5 Functions

parameter	value
fmmob	6.256×10^5
fmdry	0.1755
epdry	1×10^5
fmcap	0.0002
epcap	2.28

Table 6. fmdry Values for Each AOS Concentration

C_s [wt %]	fmdry
0.008	0.2269
0.1	0.1960
0.5	0.1817
1	0.1755
1.5	0.1696

It is therefore concluded from Figure 6 that the effect of surfactant concentration should be reflected in the fmdry parameter. Figure 7 shows the dependency of the fmdry value on the concentration of the AOS surfactant and a fitted power-law equation using the base case fmdry value (0.1755) and a fitting exponent of 0.054.

5. CONCLUSIONS

In this study, the effect of surfactant concentration on the transient and steady-state foam behaviors in porous media was investigated. Several core flood experiments were conducted, in which the nitrogen gas and solutions with different surfactant concentrations were simultaneously injected into a Bentheimer sandstone core. Moreover, the ability of the current foam models in simulating the effect of surfactant concentration was examined and modifications were suggested
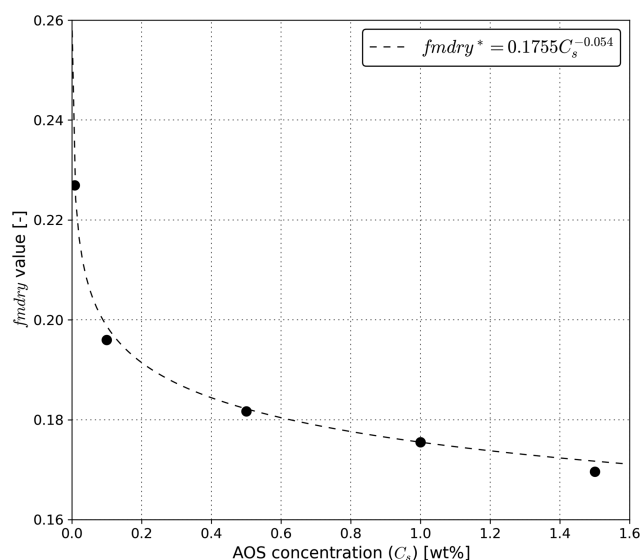
Figure 7. fmdry variations as a function of the AOS concentration.

accordingly. For the cases investigated and under our experimental conditions, the following conclusions are made:

- Strong foams can be generated with a very low surfactant concentration in the low-quality regime, albeit with a very slow generation rate.
- Surfactant concentration has a significant influence on the transient foam behavior or foam generation. The rate of foam generation increases with the increase of the surfactant concentration.
- The transition from coarse to strong foam occurs earlier as the surfactant concentration increases.
- Surfactant concentration does not impact the steady-state behavior of foam in the low-quality regime.
- In the high-quality regime, the foam strength increases with the increasing surfactant concentration. This is attributed to the influence of the limiting capillary on foam stability in this regime, whose value increases with the increase in the surfactant concentration.
- The current formulation of the steady-state implicit-textured foam models is unable to model the effect of the surfactant concentration because the current model scales both high- and low-quality regimes with the surfactant concentration.
- The only surfactant-dependent parameter in IT foam models is the limiting water saturation or the fmdry parameter. Therefore, the effect of the surfactant concentration can be reflected solely by the fmdry parameter and there is no need for a separate surfactant-concentration function.

AUTHOR INFORMATION

Corresponding Author
*E-mail: R.Farajzadeh@tudelft.nl.

ORCID ⊙
R. Farajzadeh: 0000-0003-3497-0526

Notes
The authors declare no competing financial interest.

REFERENCES

(1) Fried, A. N. *Foam-Drive Process for Increasing the Recovery of Oil*; San Francisco Petroleum Research Lab, Bureau of Mines: San Francisco, CA, 1960.

(2) Hirasaki, G.; Lawson, J. Mechanisms of foam flow in porous media: apparent viscosity in smooth capillaries. *Soc. Pet. Eng. J.* **1985**, *25*, 176−190.

(3) Kovscek, A.; Radke, C. Fundamentals of Foam Transport in Porous Media. In *Foams: Fundamentals and Applications in the Petroleum Industry*; Lawrence Berkeley Lab.: Berkeley, CA, 1994; pp 115−163.

(4) Rossen, W. R. *Foams in Enhanced Oil Recovery. Foams: Theory, Measurement, and Applications*; Prud'Homme, R. K., Khan, S., Eds.; Marcel Dekker: New York, 1996.

(5) Turta, A. T.; Singhal, A. K. *Field Foam Applications in Enhanced Oil Recovery Projects: Screening and Design Aspects*, Paper presented at the SPE International Oil and Gas Conference and Exhibition in China, 1998.

(6) Eftekhari, A. A.; Krastev, R.; Farajzadeh, R. Foam stabilized by fly ash nanoparticles for enhancing oil recovery. *Ind. Eng. Chem. Res.* **2015**, *54*, 12482−12491.

(7) Worthen, A. J.; Bagaria, H. G.; Chen, Y.; Bryant, S. L.; Huh, C.; Johnston, K. P. Nanoparticle-stabilized carbon dioxide-in-water foams with fine texture. *J. Colloid Interface Sci.* **2013**, *391*, 142−151.

(8) Khatib, Z. I.; Hirasaki, G. J.; Falls, A. H. Effects of Capillary Pressure on Coalescence and Phase Mobilities in Foams Flowing Through Porous Media. *SPE Reservoir Eng.* **1988**, *3*, 919−926.

(9) Farajzadeh, R.; Lotfollahi, M.; Eftekhari, A.; Rossen, W.; Hirasaki, G. Effect of permeability on implicit-texture foam model parameters and the limiting capillary pressure. *Energy Fuels* **2015**, *29*, 3011−3018.

(10) Apaydin, O. G.; Kovscek, A. R. Surfactant concentration and end effects on foam flow in porous media. *Transp. Porous Media* **2001**, *43*, 511−536.

(11) Aronson, A.; Bergeron, V.; Fagan, M. E.; Radke, C. The influence of disjoining pressure on foam stability and flow in porous media. *Colloids Surf., A* **1994**, *83*, 109−120.

(12) Marsden, S.; Khan, S. A. The flow of foam through short porous media and apparent viscosity measurements. *Soc. Pet. Eng. J.* **1966**, *6*, 17−25.

(13) Jones, S. A.; van der Bent, V.; Farajzadeh, R.; Rossen, W. R.; Vincent-Bonnieu, S. Surfactant screening for foam EOR: Correlation between bulk and core-flood experiments. *Colloids Surf., A* **2016**, *500*, 166−176.

(14) Farajzadeh, R.; Krastev, R.; Zitha, P. Foam films stabilized with alpha olefin sulfonate (AOS). *Colloids Surf., A* **2008**, *324*, 35−40.

(15) Ma, K.; Lopez-Salinas, J. L.; Puerto, M. C.; Miller, C. A.; Biswal, S. L.; Hirasaki, G. J. Estimation of Parameters for the Simulation of Foam Flow through Porous Media. Part 1: The Dry-Out Effect. *Energy Fuels* **2013**, *27*, 2363−2375.

(16) Ma, K.; Farajzadeh, R.; Lopez-Salinas, J. L.; Miller, C. A.; Biswal, S. L.; Hirasaki, G. J. Non-uniqueness, Numerical Artifacts, and Parameter Sensitivity in Simulating Steady-State and Transient Foam Flow Through Porous Media. *Transp. Porous Media* **2014**, *102*, 325−348.

(17) Kahrobaei, S.; Vincent-Bonnieu, S.; Farajzadeh, R. Experimental Study of Hysteresis behavior of Foam Generation in Porous Media. *Sci. Rep.* **2017**, *7*, No. 8986.

(18) Bernard, G. G.; Holm, L. Effect of foam on permeability of porous media to gas. *Soc. Pet. Eng. J.* **1964**, *4*, 267−274.

(19) Eftekhari, A. A.; Farajzadeh, R. Effect of Foam on Liquid Phase Mobility in Porous Media. *Sci. Rep.* **2017**, *7*, No. 43870.

(20) Computer Modelling Group*STARS User's Guide*; Computer Modelling Group Ltd: Calgary, Alberta, Canada, 2010.

(21) Boeije, C.; Rossen, W. *Fitting Foam Simulation Model Parameters to Data*, Paper presented at the IOR 2013-17th European Symposium on Improved Oil Recovery, Saint Petersburg, Russia, 16 April, 2013.

(22) Corey, A. T. The interrelation between gas and oil relative permeabilities. *Prod. Mon.* **1954**, *19*, 38−41.

(23) Peng, D.-Y.; Robinson, D. B. A new two-constant equation of state. *Ind. Eng. Chem. Fundam.* **1976**, *15*, 59−64.

(24) Lotfollahi, M.; Farajzadeh, R.; Delshad, M.; Varavei, A.; Rossen, W. R. Comparison of implicit-texture and population-balance foam models. *J. Nat. Gas Sci. Eng.* **2016**, *31*, 184−197.